Remote Sensing of Environment 308 (2024) 114199

Contents lists available at ScienceDirect

Remote Sensing of Environment

journal homepage: www.elsevier.com/locate/rse

Using CloudSat to Advance the Global Precipitation Climatology Project (GPCP) over Antarctica

Mohammad Reza Ehsani [a,*], Ali Behrangi [a], Cristian Román-Palacios [b], George J. Huffman [c], Robert F. Adler [d]

[a] Department of Hydrology and Atmospheric Sciences, The University of Arizona, Tucson, AZ, United States of America
[b] School of Information, The University of Arizona, Tucson, AZ, United States of America
[c] Mesoscale Atmospheric Processes Laboratory, NASA Goddard Space Flight Center, Greenbelt, MD, United States of America
[d] Earth System Science Interdisciplinary Center, Cooperative Institute for Climate and Satellites, University of Maryland, College Park, MD, United States of America

ARTICLE INFO

Editor: Menghua Wang

Keywords:
CloudSat
GPCP
Antarctica
Remote sensing
Precipitation
TOVS
AIRS
ERA5

ABSTRACT

Remote sensing-based precipitation products face several challenges in high latitudes and specifically over frozen surfaces (i.e., snow and ice). Consequently, precipitation estimates tend to be lower in quality over these regions, including Antarctica, the coldest continent on Earth. In this study, we developed a method for adjusting precipitation estimates over Antarctica by leveraging CloudSat's ability to capture snowfall compared to other satellite products over snow and ice surfaces. We addressed limitations of CloudSat, such as poor spatiotemporal sampling, noise, and incomplete coverage near the poles. We utilized the European Centre for Medium-Range Weather Forecasts (ECMWF) Reanalysis 5th Generation (ERA5) to guide development, particularly during the period when the TIROS Operational Vertical Sounder (TOVS) was contributing. We adjusted monthly and seasonal TOVS and Atmospheric Infrared Sounder – Infrared (AIRS-IR) precipitation biases over Antarctica at the pixel level, as these two products are the primary inputs for the Global Precipitation Climatology Project (GPCP) in high latitudes. We assessed the adjusted TOVS and AIRS-IR through analyses of geographical maps and time series of monthly and seasonal mean precipitation rates. The results are encouraging, indicating that the proposed approach could replace the current approach used in the GPCP for adjusting precipitation estimates from AIRS-IR and TOVS over Antarctica. Adjusting precipitation estimates from TOVS and AIRS-IR using the proposed approach improves the Kling-Gupta efficiency (KGE) over their entire period by 162% and 147%, respectively. Moreover, the proposed approach can be applied to adjust other precipitation products over Antarctica at the pixel level, including satellites and reanalysis products.

1. Introduction

Remote sensing enables researchers to collect critical information about the Earth from a distance. For instance, it facilitates the mapping of large forest fires from space, providing rangers with a broader view of the affected area compared to ground-level observations. Additionally, remote sensing aids in studying clouds, which contributes to improved weather prediction. As remote sensing techniques advance, we can now estimate global precipitation, a crucial element of the hydrological cycle.

Remote sensing precipitation products offer a solution to some of the shortcomings associated with traditional in-situ (gauge-based) products which suffer from sparsity. These products incorporate data from diverse instruments, including radar (Seto et al., 2022), passive microwave (PMW, Adhikari et al., 2020; Kummerow et al., 1996), and thermal infrared (IR) imagers and sounders (Ehsani et al., 2021; Kidd and Huffman, 2011; Susskind et al., 1997). However, remote sensing precipitation products may introduce biases due to systematic and random errors in their retrieval algorithms (Ehsani et al., 2022a), limited temporal sampling (Behrangi and Wen, 2017; Sun et al., 2018), and relatively lower accuracy over frozen surfaces (Arabzadeh et al., 2020; Ehsani et al., 2022b; Ehsani and Behrangi, 2022; Ferraro et al., 2013; Song et al., 2021; Broxton et al., 2024). Furthermore, relatively short data records of remote sensing products can affect the accuracy of these

* Corresponding author.
E-mail addresses: rehsani@arizona.edu (M.R. Ehsani), behrangi@arizona.edu (A. Behrangi), cromanpa94@arizona.edu (C. Román-Palacios), george.j.huffman@nasa.gov (G.J. Huffman), radler@umd.edu (R.F. Adler).

https://doi.org/10.1016/j.rse.2024.114199
Received 26 July 2023; Received in revised form 30 April 2024; Accepted 3 May 2024
Available online 9 May 2024

products (Sadeghi et al., 2019).

Snow is the primary form of precipitation in higher latitudes and polar regions. Accurate quantification of precipitation in these areas is crucial for comprehending Earth's current climate status and cryosphere studies (Hoopes et al., 2023). The accumulated snowpack serves as a significant freshwater resource for numerous countries, underscoring the importance of precise high-latitude snowfall assessment at both regional and global scales. Nevertheless, satellite remote sensing encounters several challenges when estimating high-latitude precipitation. These challenges include poor sensitivity of sensors to light rain and snowfall, resulting in substantial missing or underestimated precipitation (Behrangi et al., 2012; Berg et al., 2006; Lebsock and L'Ecuyer, 2011). Moreover, the unknown surface emissivity over snow and ice surfaces (Ferraro et al., 2013) adds to the complexity of the retrieval process.

Antarctica, the coldest continent on Earth, poses severe challenges due to its frigid climate and snow-covered landscape. With an ice-cap climate and temperatures reaching as low as −90 °C during winter, the majority of the continent remains covered in an immense ice sheet, nearly 1.6 km thick, accounting for 98% of its surface. The presence of katabatic winds limits weather fronts from penetrating far into the continent. Previous studies have shown potential underestimation of snowfall accumulation over this region and consequently, there is a pressing need to identify new resources to improve precipitation estimates in Antarctica's extreme and predominantly dry conditions.

Due to the severe climate and maintenance difficulties, in-situ measurements of precipitation in Antarctica are extremely limited (Seefeldt et al., 2021), to the point that the Global Precipitation Climatology Centre (GPCC; Schneider et al., 2017) cannot construct a reliable analysis of this region. As a result, the satellite-gauge Global Precipitation Climatology Project (GPCP; Huffman et al., 2023) that uses GPCC for bias correction over land, lacks gauge input over Antarctica. So far, GPCP has relied on precipitation estimates from the Atmospheric Infrared Sounder (AIRS) and TIROS Operational Vertical Sounder (TOVS), mainly due to the poor performance and relatively short record of PMW sensors, and lack of coverage from geostationary infrared satellites over Antarctica. Due to the large underestimation of precipitation from AIRS and TOVS over Antarctica, GPCP utilizes a constant adjustment factor (i.e., ≈1.4; based on some limited gauge analyses) to reduce the precipitation bias. However, this approach is not very accurate and ignores regional corrections.

Recent research has demonstrated that CloudSat presents a promising alternative for analyzing regional and global snowfall and assessing precipitation estimates in high latitudes including Antarctica (Behrangi et al., 2016; Behrangi et al., 2014b; Behrangi et al., 2014a; Kulie et al., 2016; Liu, 2008; Palerme et al., 2014a, 2014b). Previous evaluations of CloudSat's precipitation products have shown promising results, highlighting its strong ability to detect falling snow from space. In a study by Behrangi et al. (2020), the annual snow accumulation measured by CloudSat was compared with mass change observations from the Gravity Recovery and Climate Experiment (GRACE) over seven Antarctic basins, revealing good agreement between the two observational products. This agreement enhances confidence in CloudSat's capability to accurately capture snowfall accumulation, particularly on an annual basis (Behrangi et al., 2019).

Nevertheless, CloudSat's estimates are not without challenges (Arthern et al., 2006). One notable issue is its inability to capture precipitation near the surface due to interference from ground clutter (Battaglia and Panegrossi, 2020; Bennartz et al., 2019; Skofronick-Jackson et al., 2019; Smalley et al., 2017). Moreover, CloudSat's coverage is limited temporally (spanning from 2006 to 2010) and geographically (no observations are available poleward of 82°). Additionally, CloudSat's narrow swaths (and nadir observations) result in poor sampling. Some studies have attempted to address some of these drawbacks associated with CloudSat. For instance, Grazioli et al. (2017) employed a combination of new in-situ data collected along the coast of Adelie Land over one year, revealing that about 17% of falling snow sublimates before reaching the surface due to dry air in the lower troposphere. Since CloudSat's snowfall estimate is made at approximately 1.2 km above the surface to avoid surface clutter (Tanelli et al., 2008), it is likely less affected by the reduced snowfall rate due to the sublimation. Grazioli et al. (2017) demonstrated the possibility of compensating for some of the precipitation missed by CloudSat using the reanalysis vertical profile of precipitation.

Reanalysis datasets like the European Centre for Medium-Range Weather Forecasts (ECMWF) Reanalysis 5th Generation (ERA5) provide extended temporal coverage compared to CloudSat and other remote sensing products. Nevertheless, the reliability of reanalysis products raises concerns primarily due to their reliance on numerical models, which often lead to an overestimation of precipitation over Antarctica (Palerme et al., 2017). Additionally, the assimilation of observations may not fully address all the modeling issues. Inherent uncertainties in reanalysis products pose challenges in terms of comprehension and quantification (Ghajarnia et al., 2022).

In this study, we develop a new climatology product based on CloudSat over Antarctica (hereafter CloudSat-Antarctica) that addresses some of the limitations of CloudSat. The main objective is to use more-reliable precipitation climatology estimates of CloudSat-Antarctica to create spatiotemporal correction factors. These correction factors then can be applied to adjust precipitation estimates by individual or combined sensor products such as GPCP and the Integrated Multi-satellitE Retrievals for the Global Precipitation Measurement (GPM) mission (IMERG; Huffman et al., 2020) over Antarctica. In the following sections, datasets, and methodology are described first, then the results are presented and discussed, followed by concluding remarks.

2- Study area, datasets, and methodology

1.1. Datasets

1.1.1. CloudSat

Nadir-looking CloudSat cloud profiling radar, operating at 94-GHz on the CloudSat satellite, measures the radar backscatter from clouds and other objects at varying distances from the radar. It offers cross-track, along-track, and vertical resolutions of 1.4 km, 1.7 km, and 0.5 km, respectively, covering the latitude range from 82°S to 82°N. For this study, the 2C-SNOW-PROFILE V05 product, which provides near-surface snowfall rates was utilized. The 2C-SNOW-PROFILE product demonstrates satisfactory performance over land areas (Smalley et al., 2017). Nevertheless, some limitations affect CloudSat's accuracy in measuring intense surface snowfall rates, mainly related to attenuation issues and ground clutter (Battaglia and Panegrossi, 2020; Bennartz et al., 2019; Skofronick-Jackson et al., 2019; Stephens et al., 2002). Additionally, from 2011 onwards, battery constraints restricted CloudSat's sampling to daytime only, leading to a significant reduction in observations over Antarctica (Milani and Wood, 2021). Thus, this study focuses on CloudSat data from the period of 2007 to 2010 when both day and night observations were available. In this study, CloudSat is regridded into a 0.5° level-3 grid over Antarctica to match the spatial resolution of GPCP V3.2 using a binning method.

1.1.2. ERA5

ERA5 offers hourly computations for numerous climate variables related to the atmosphere, land, and oceans. These calculations are performed on a 30-km grid, and the atmosphere is represented with 137 levels extending from the Earth's surface up to 80 km in height. To generate these estimates, ERA5 integrates extensive historical weather observations worldwide through sophisticated modeling and data assimilation techniques (Hersbach et al., 2020). This study combines ERA5's convective and large-scale snowfall rates to conduct a comparison with other snowfall products, thereby evaluating the total snowfall. Similar to CloudSat, ERA5 is regridded into a 0.5° grid using bivariate spline approximation.

Table 1
Summary of precipitation products used in this study.

Product	Period	Spatial Resolution
CloudSat	Jan 2007 - Dec 2010	0.5°
ERA5	Jan 1983 - Dec 2020	0.5°
TOVS	Jan 1983 - Aug 2002	0.5°
AIRS-IR	Sep 2002 - Dec 2020	0.5°

1.1.3. TOVS

The TOVS precipitation dataset is derived using the methodology described by Susskind et al. (1997). This approach utilizes a climatological multiple regression relationship between rain gauge measurements and various TOVS-based parameters related to cloud volume, cloud-top pressure, fractional cloud cover, and relative humidity profile. Specifically, cloud properties extracted from TOVS are translated into precipitation values through regression analysis against the First Global Atmospheric Research Program (GARP) Global Experiment rain stations. This relationship is allowed to vary both seasonally and latitudinally, with separate relationships established for ocean and land areas. The TOVS precipitation dataset serves as an input in the GPCP merged dataset (Huffman et al., 2023). For this study, TOVS data were obtained from the GPCP input package, where the data was rescaled from 1° resolution to 0.5° through grid box replication, and histogram-matching was employed to calibrate the TOVS precipitation estimates to AIRS in three different segments (Huffman et al., 2023).

1.1.4. AIRS

Aboard the Earth Observing System Aqua satellite, AIRS operates as an infrared sounder. One of AIRS's primary goals is to provide temperature and humidity profiles, along with various other atmospheric products, in conjunction with observations from the Advanced Microwave Sounding Unit (AMSU) and the Humidity Sounder for Brazil (HSB). The precipitation retrieval method introduced by Susskind et al. (1997), which is employed for TOVS data, is also applied to AIRS data. However, due to the loss of AMSU-A2 in 2016, a modified version of the algorithm called AIRS-IR was developed, utilizing only infrared data. This modified version is applied to the entire AIRS record to maintain consistency. GPCP utilizes precipitation retrievals based on this AIRS-IR at 0.5° spatial resolution, and the same version is utilized in the current study as well (Table 1).

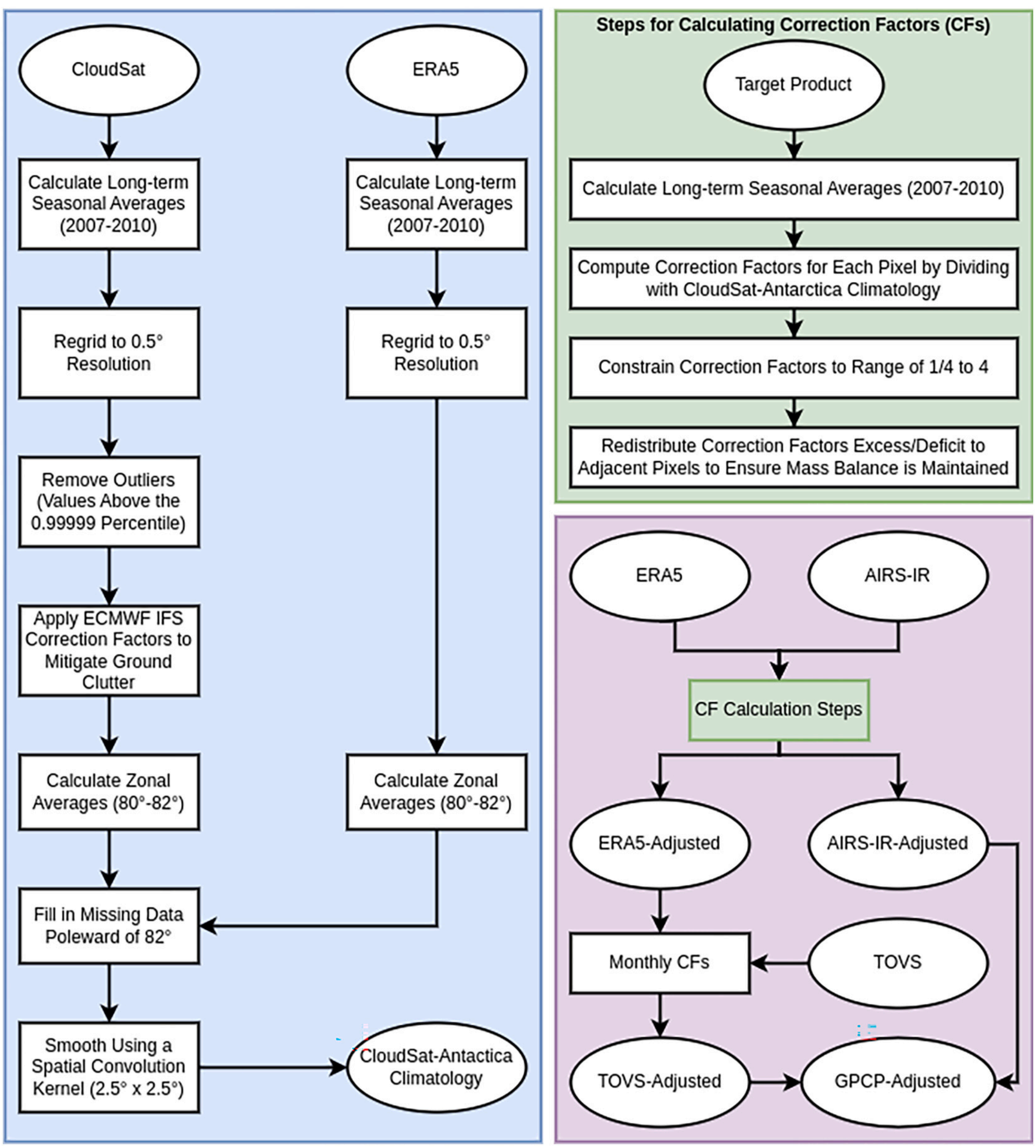

Fig. 1. Flowchart explaining how correction factors are calculated.

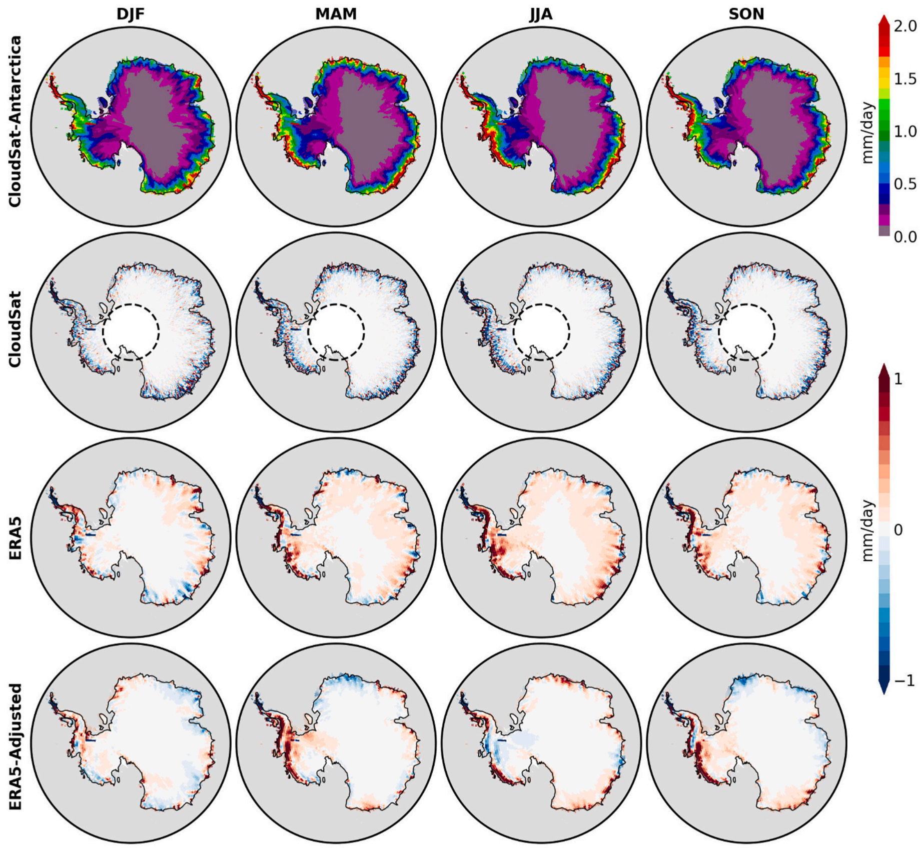

Fig. 2. First row: Seasonal precipitation maps of CloudSat-Antarctica in mm/day. Second to fourth rows: difference between the long-term (2007–2010) seasonal averages of CloudSat, ERA5, and ERA5-Adjusted and CloudSat-Antarctica seasonal climatology in mm/day. Red/blue colors indicate over/underestimation, respectively. (For interpretation of the references to colour in this figure legend, the reader is referred to the web version of this article.)

1.2. Methodology

The main objective of this study is to develop a new approach for adjusting TOVS and AIRS-IR over Antarctica (as the main inputs to the GPCP) utilizing more advanced snowfall estimates from CloudSat to replace the simple legacy adjustment method currently used in GPCP V3.2 and later used in other products such as IMERG V07. Before their use in GPCP V3.2, the inter-calibrated TOVS, and AIRS-IR are currently adjusted by a constant climatological factor (i.e., ≈1.4) based on some limited gauge analysis. This approach is insufficient because a constant adjustment factor fails to address regional precipitation patterns and biases, as well as spatiotemporal variations. Therefore, we proposed a new pixel-level method that can adjust precipitation patterns and rates, regionally and over the entire Antarctica (Cabaj et al., 2020; King and Fletcher, 2021).

The proposed approach, summarized in, uses the four-year (i.e., 2007–2010) regionally and seasonally varying CloudSat climatology and derives adjustments to force various other estimates to closely mimic the CloudSat climatology on the pixel level. The correction factors are computed for both land and ocean and applied over the Antarctic ice sheet (as shown in the geographical maps), but they can easily be extended to ice shelves and off-shore.

The first step in generating the CloudSat-Antarctica climatology product was to calculate the long-term seasonal averages of CloudSat. The seasonal averages were then re-gridded to a 0.5° spatial resolution regular grid to match the resolution of GPCP, AIRS-IR, and TOVS products using a simple binning approach. Outlier precipitation estimates (>99.9999% of the estimates over Antarctica) were removed for each season. Similar to Grazioli et al. (2017), ECMWF Integrated Forecast System (IFS) was used to calculate adjustment factors for CloudSat to account for ground-clutter. For this purpose, the cumulative precipitation near the surface was divided by precipitation accumulation at 1.2 km above the surface and applied to the CloudSat climatology.

Similarly, the long-term seasonal averages of ERA5 were calculated and re-gridded to a 0.5° spatial resolution using bivariate spline approximation. These averages were then used to fill CloudSat gaps poleward of 82°S. For the gap-filling step, the ratio of seasonal averages of CloudSat and ERA5 for 80°S-82°S was calculated first and then applied to ERA5 poleward of 82°S to estimate CloudSat precipitation across the gap. It is noteworthy to mention that for the 2007–2010 period, our methodology primarily leverages CloudSat data, with ERA5 playing a supplementary role in filling spatial gaps poleward of 82°, where precipitation is almost negligible. It's worth noting that in this context, ERA5 contributes a minor portion (approximately 4.1%) to the weighted pixel precipitation, underscoring that the core of our adjustments and analysis is rooted in CloudSat observations.

Lastly, a smoothing operation was applied to minimize noise in the final CloudSat-Antarctica product. The smoothing step includes convolving the precipitation estimates using a 5 × 5 kernel/filter that takes the average of the neighboring pixels and applies that to the center pixel. The CloudSat-Antarctica seasonal climatology product was then used to calculate pixel-based (0.5°) correction factors to adjust other precipitation products over Antarctica. This step includes dividing the CloudSat-Antarctica product by the target product and then constraining the correction factors to the range of 1/4 to 4 by re-distributing the extra weights to neighboring pixels to make sure that zonal-averages over the entire Antarctica is close to one. This range is adapted after trial and error experiments with the goal to avoid overly large changes in the original product.

The first correction factors were calculated for the ERA5 precipitation product. ERA5 seasonal precipitation data was then multiplied by

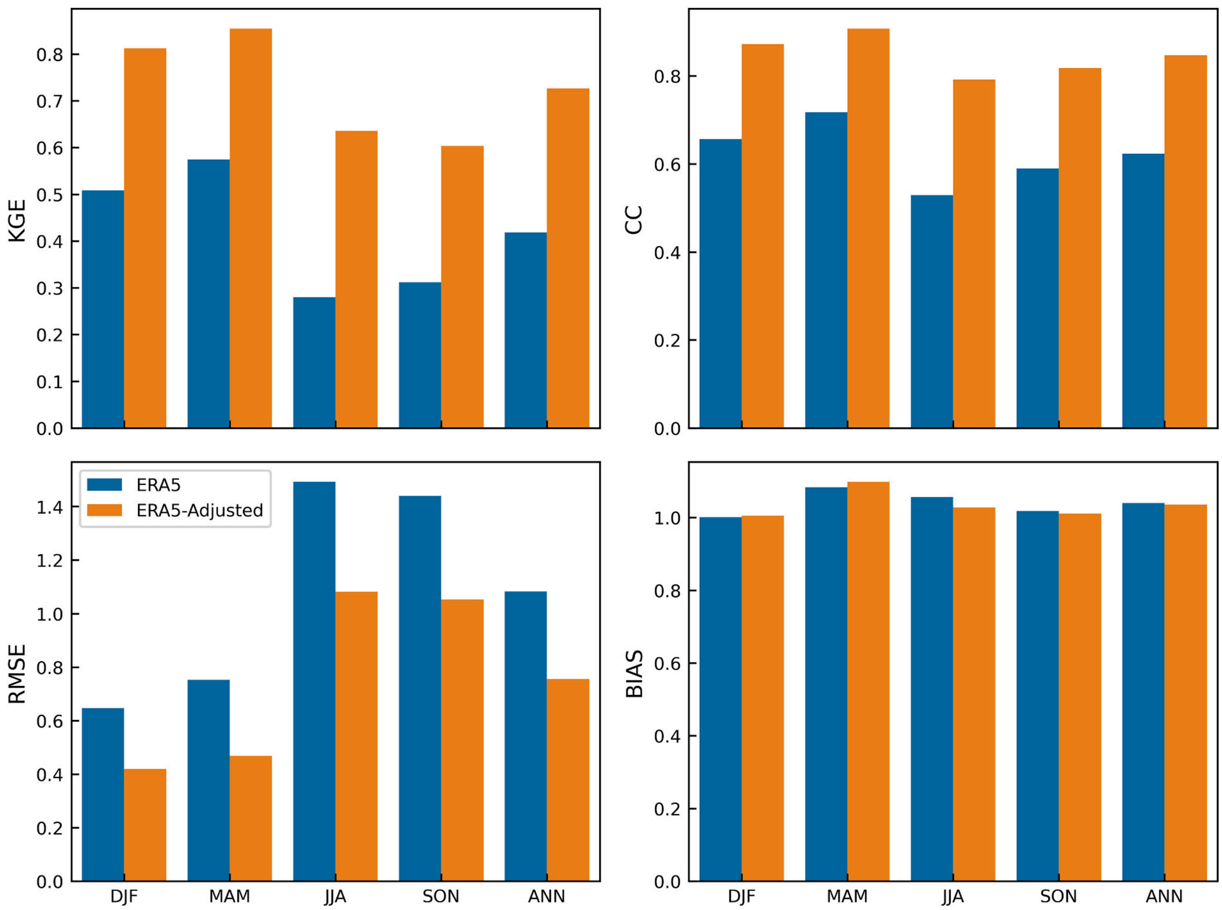

Fig. 3. Summary of statistics for ERA5 and ERA5-Adjusted based on Fig. 2.

corresponding seasonal correction factors to create the ERA5-Adjusted product. ERA5-Adjusted was then compared with CloudSat, CloudSat-Antarctica, and ERA5 for the period 2007–2010 to evaluate the efficiency of the proposed approach during the 2007–2010 period.

Before calculating the correction factors for TOVS and AIRS-IR products, an extensive statistical analysis was performed comparing the two products. With this analysis, we noticed that there is a shift in the zonal averages between TOVS and AIRS-IR periods (0.42 vs 0.37 mm/day). Seasonal and monthly time series showed that TOVS has a different spatiotemporal precipitation pattern and long-term average than AIRS-IR, so static correction factors based on the climatology of CloudSat-Antarctica could not be directly applied to TOVS period. To overcome this issue, we first adjusted ERA5 precipitation with CloudSat-Antarctica for the TOVS period and then used ERA5-Adjusted to adjust TOVS on a month-by-month and season-by-season basis (that is dividing ERA5-Adjusted by TOVS for each month/season and then multiplying TOVS values by that factor for each pixel). Conversely, climatological correction factors derived from CloudSat-Antarctica were directly applied to adjust the bias of AIRS-IR, as the time-series of AIRS-IR was found to align well with CloudSat and ERA5 time-series.

Since correction factors are calculated for seasons, but the precipitation data are monthly, we choose monthly correction factors to be identical for each month of the season. For example, for DJF, the same correction factors are applied to December, January, and February. In a separate set of experiments (not included in the manuscript), we developed monthly correction factors from the monthly CloudSat-Antarctica climatology product with a similar methodology. However, considering the limitations of the CloudSat, specifically poor spatio-temporal sampling, the monthly CloudSat-Antarctica climatology product did not improve the monthly time-series of the investigated products as effectively as seasonal CloudSat-Antarctica applied to monthly data. Therefore, we decided to use seasonal correction factors on both monthly and seasonal time-series.

A series of analyses were performed to compare TOVS, AIRS-IR, ERA5, and their adjusted versions (TOVS-Adjusted, AIRS-IR-Adjusted, and ERA5-Adjusted, respectively). Statistical metrics and analyses were used to quantify the changes after applying correction factors. Finally, GPCP V3.2, which uses TOVS and AIRS-IR by a constant adjustment factor was reconstructed with the TOVS-Adjusted and AIRS-IR-Adjusted to demonstrate/evaluate the impact of the proposed methodology. Flowchart in Fig. 1 summarizes the methodology of the present study.

2. Results

In the first experiment, the CloudSat-Antarctica climatology product was compared with corresponding seasonal averages of CloudSat, ERA5, and ERA5-Adjusted for the period 2007–2010. ERA5-Adjusted is the ERA5 product adjusted by pixel-based correction factors based on CloudSat-Antarctica. Fig. 2 shows the advantages of CloudSat-Antarctica compared to CloudSat. Gaps poleward of 82°S are filled and the patterns are less noisy. As detailed in Fig. 3, ERA5-Adjusted shows patterns that are similar to CloudSat-Antarctica, which is reflected in higher KGE (Kling-Gupta Efficiency; 0.73 in all seasons) compared to ERA5 (0.42). Applying correction factors also improves the correlation coefficient (CC) of ERA5-Adjusted (0.85) compared to ERA5 (0.62), decreases the root mean squared difference (RMSD; 0.76 vs 1.08 mm/day), and reduces the bias of the ERA5-Adjusted with respect to CloudSat-Antarctica in all seasons compared to the bias ratio of the ERA5 original product (1.01 vs 1.03). Note that the statistics are not

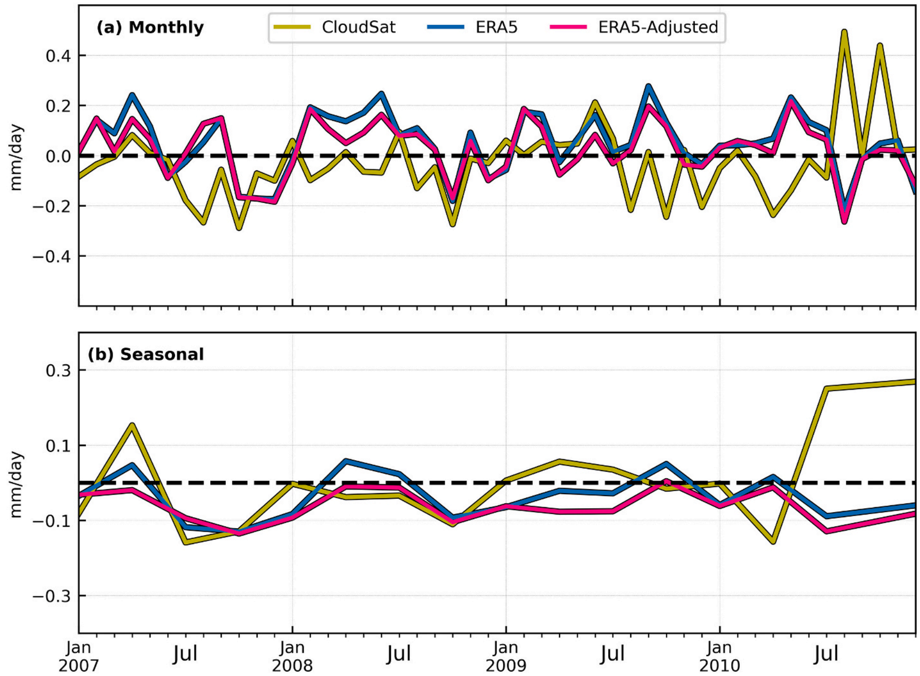

Fig. 4. (a) Monthly and (b) seasonal time series of Antarctic average snowfall from CloudSat, ERA5, and ERA5-Adjusted products relative to CloudSat-Antarctica for the period 2007–2010 in mm/day. The average snowfall rates are only calculated down to 82°S for consistency between CloudSat and other products.

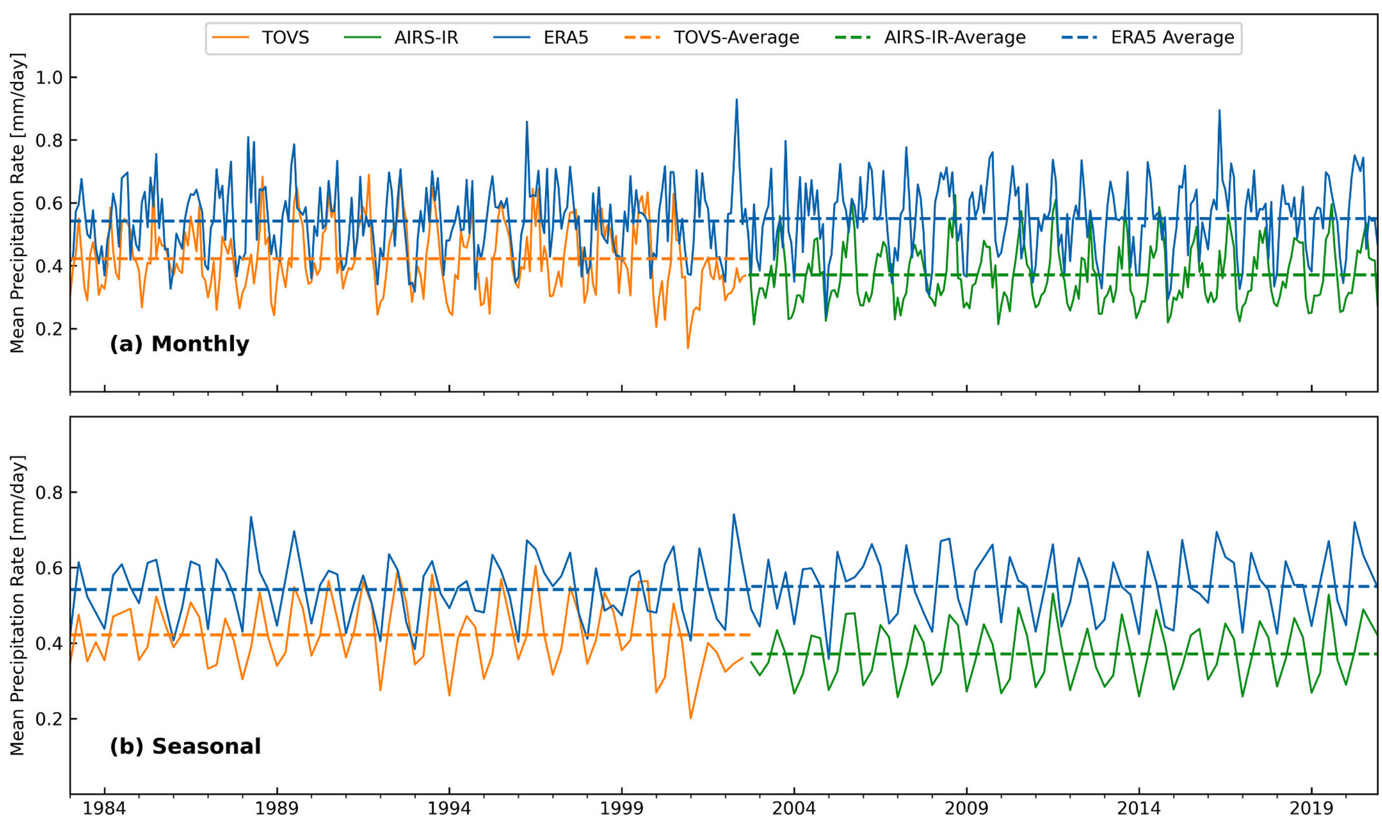

Fig. 5. a) Monthly and b) seasonal time series of Antarctic average precipitation from TOVS, AIRS-IR, ERA5, and their long-term averages (dashed lines) in mm/day.

appreciably affected by the region poleward of 82°S since it contains zero or near-zero precipitation values. The visual assessment of Fig. 2 also shows improvement in the ERA5-Adjusted precipitation patterns compared to the ERA5. This indicates that correction factors can effectively improve both precipitation patterns and statistical metrics.

Fig. 4 shows monthly (Fig. 4a) and seasonal (Fig. 4b) average snowfall rates over Antarctica from ERA5, ERA5-Adjusted, and CloudSat relative to CloudSat-Antarctica. Since CloudSat precipitation products do not cover 82°S-90°S, the average snowfall rates are only calculated down to 82°S for consistency between CloudSat and other products. This

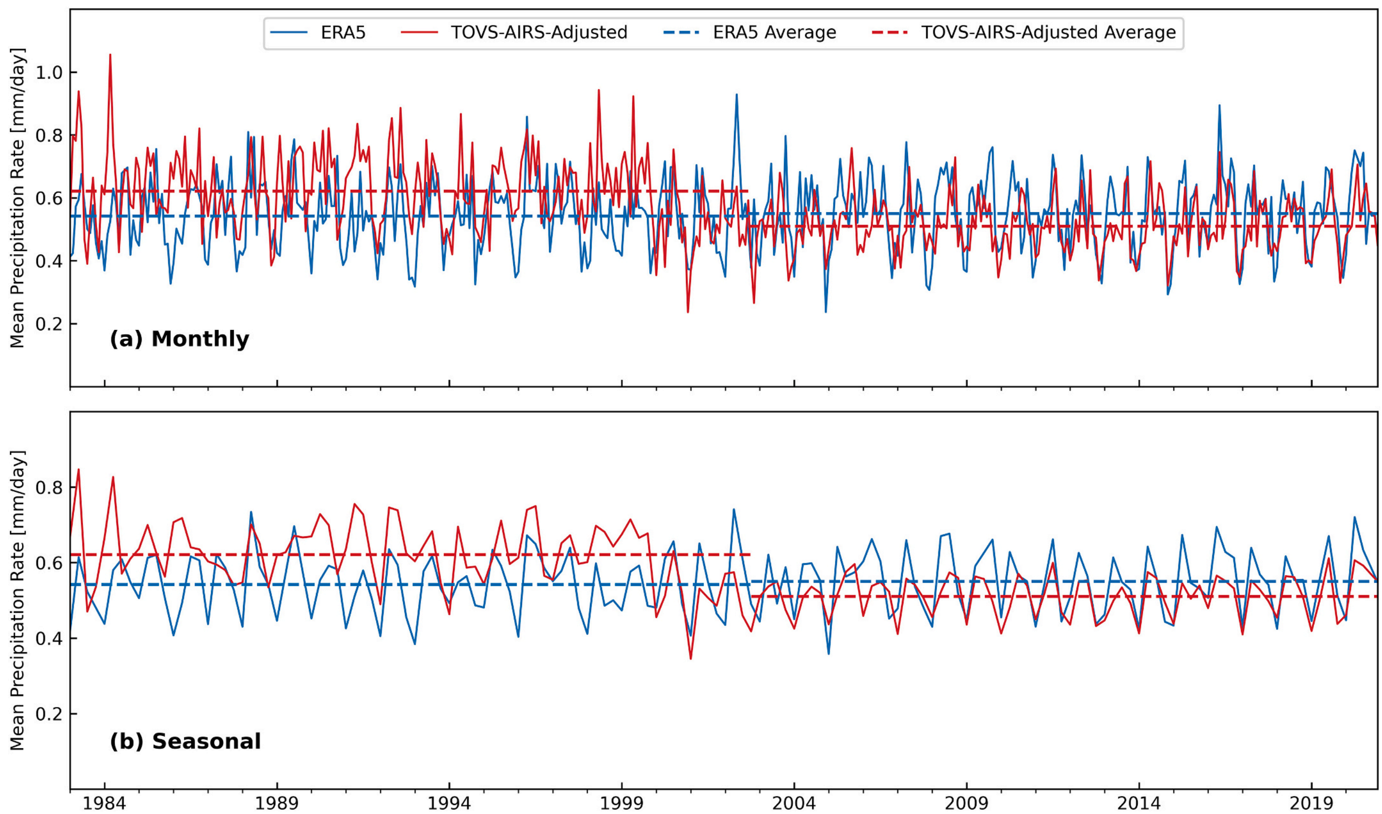

Fig. 6. a) Monthly and b) seasonal time series of Antarctic average precipitation from ERA5 and TOVS-AIRS adjusted by static correction factors, and their long-term averages (dashed lines) in mm/day.

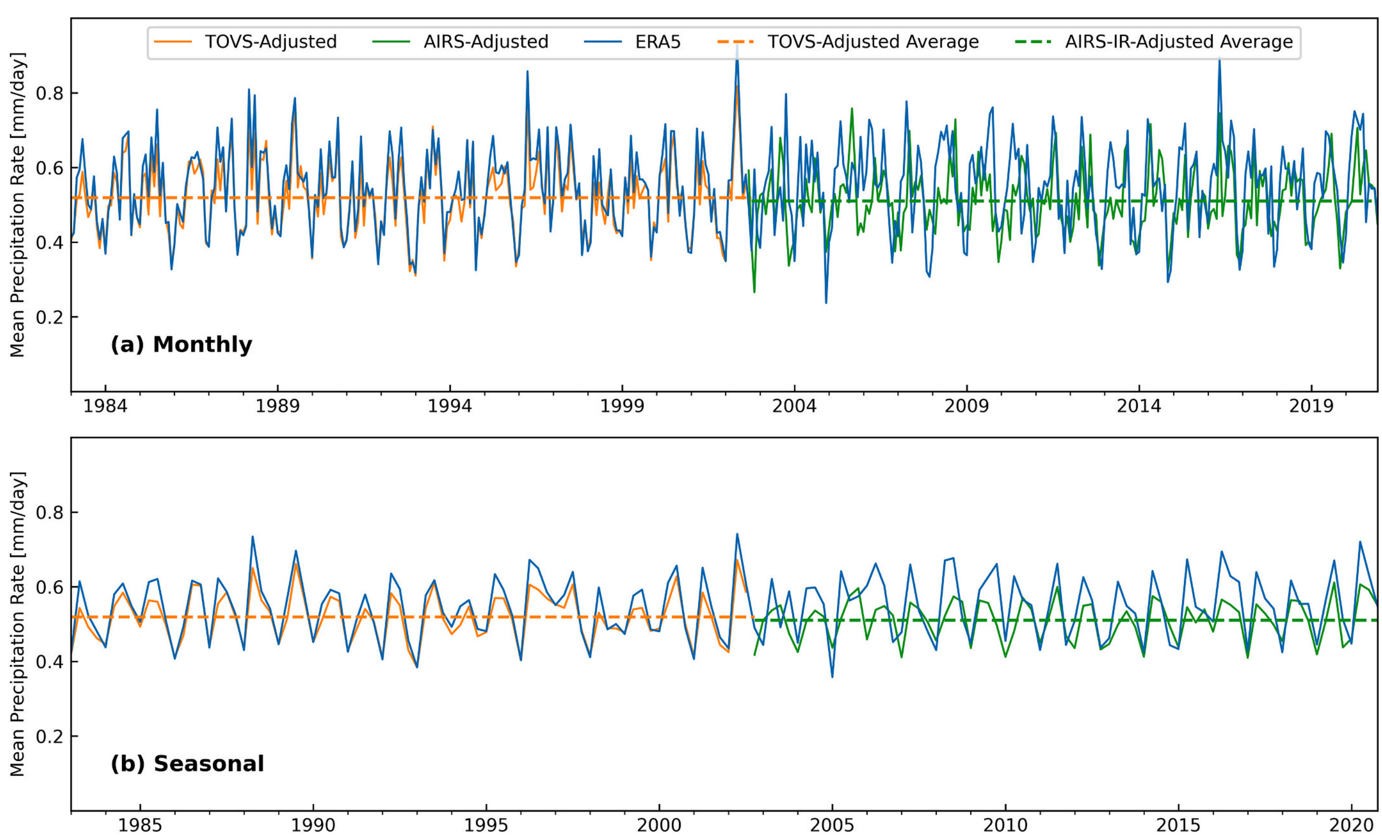

Fig. 7. a) Monthly and b) seasonal time series of Antarctic average precipitation from TOVS-Adjusted, AIRS-IR-Adjusted, and ERA5 and the long-term averages (dashed lines) of adjusted products all in mm/day.

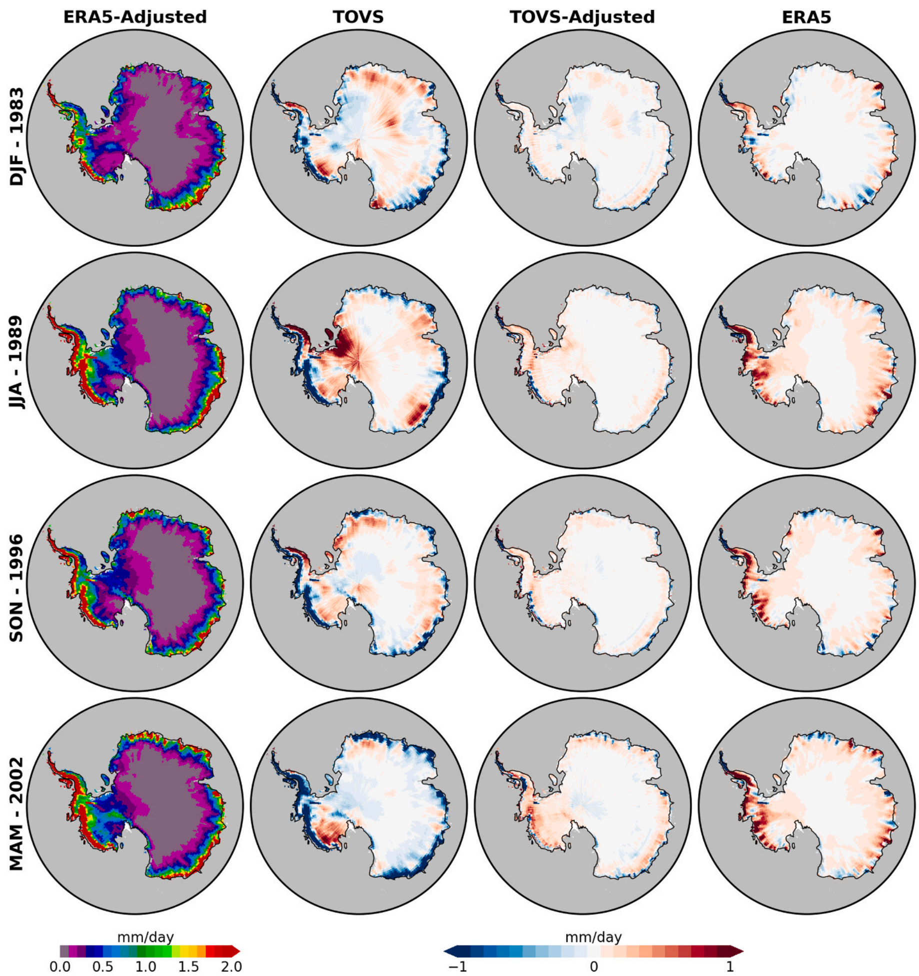

Fig. 8. Seasonal maps of precipitation rates for four case studies (each for one separate season) sampled from the TOVS period: First column on the left: map of mean precipitation from ERA5-Adjusted (i.e., the reference), Second through fourth columns: Maps of precipitation values from the other products (TOVS, TOVS-Adjusted, ERA5) minus ERA5-Adjusted.

experiment investigates if the proposed approach that uses long-term climatological averages to drive correction factors cause any peculiar pattern in monthly and seasonal time-series of the adjusted product (in this case ERA5-Adjusted).

Visual assessment of the ERA5-Adjusted and ERA5 time series at both seasonal and monthly time scales indicates that applying correction factors makes ERA5-Adjusted more similar to CloudSat-Antarctica (as expected) which is reflected in the improved KGE (0.63 vs 0.32) as a general metric that incorporate correlation, bias and variability ratio. This experiment indicates that though correction factors are static/fixed (i.e., calculated based on the long-term seasonal climatology of CloudSat-Antarctica and ERA5), are effective in improving the monthly/seasonal time series of ERA5-Adjusted (that visually is reflected in being closer to horizontal dashed line at zero).

Fig. 5 shows the time series of TOVS, AIRS-IR, ERA5, and their long-term averages (dashed lines). TOVS and AIRS have different long-term averages (0.42 vs 0.37 mm/day for seasonal time-series). The long-term averages of ERA5 for the TOVS and AIRS-IR periods of record (approximately 0.55 mm/day, dashed blue line) indicate that there should not be a large difference between the TOVS and AIRS-IR averages. Statistical tests, for example Augmented Dickey-Fuller Test, indicate that TOVS has a trend (ADF Statistic: -1.7, p-value: 0.44), while this is not the case for AIRS-IR. Furthermore, TOVS precipitation has lower spatial resolution and lower quality compared to AIRS-IR, leading to different zonal precipitation averages between the two products (discussed below in the case studies experiments).

As mentioned earlier, the correction factors based on the CloudSat-Antarctica climatology product are calculated for the 2007–2010 period, when CloudSat-Antarctica and AIRS-IR overlap. Side studies showed that adjusting TOVS by the climatological CloudSat-Antarctica correction factors results in unreasonably large values and variations. The TOVS-Adjusted Average value also becomes much larger than the AIRS-Adjusted Average value, making the TOVS-AIRS time series even less consistent (0.62 vs 0.51 mm/day for TOVS and AIRS-IR periods respectively; Fig. 6).

To overcome this issue, TOVS' precipitation patterns and trends in both monthly and seasonal time series need to be improved before any adjustment. Because CloudSat is not available for the TOVS period, ERA5-Adjusted was used to compute dynamic correction factors (i.e., varying monthly/seasonally) for adjusting TOVS. This was not needed for AIRS-IR, as AIRS-IR shows a pattern that compares well to CloudSat-Antarctica, so correction factors based on CloudSat-Antarctica were directly applied to AIRS-IR.

Fig. 7 shows the time series of ERA5, TOVS-Adjusted, and AIRS-IR-Adjusted in both monthly and seasonal scales. A visual comparison between Fig. 6 and Fig. 7 suggests that TOVS-Adjusted is now a better match to the AIRS-IR time-series, in terms of both magnitude and variation. The dynamic correction factors approach applied to TOVS seems to be effective, leading to long-term averages of TOVS-Adjusted and AIRS-IR-Adjusted that almost coincide.

Apart from time-series of monthly/seasonal average, it is important to evaluate the impacts of the correction factors on regional

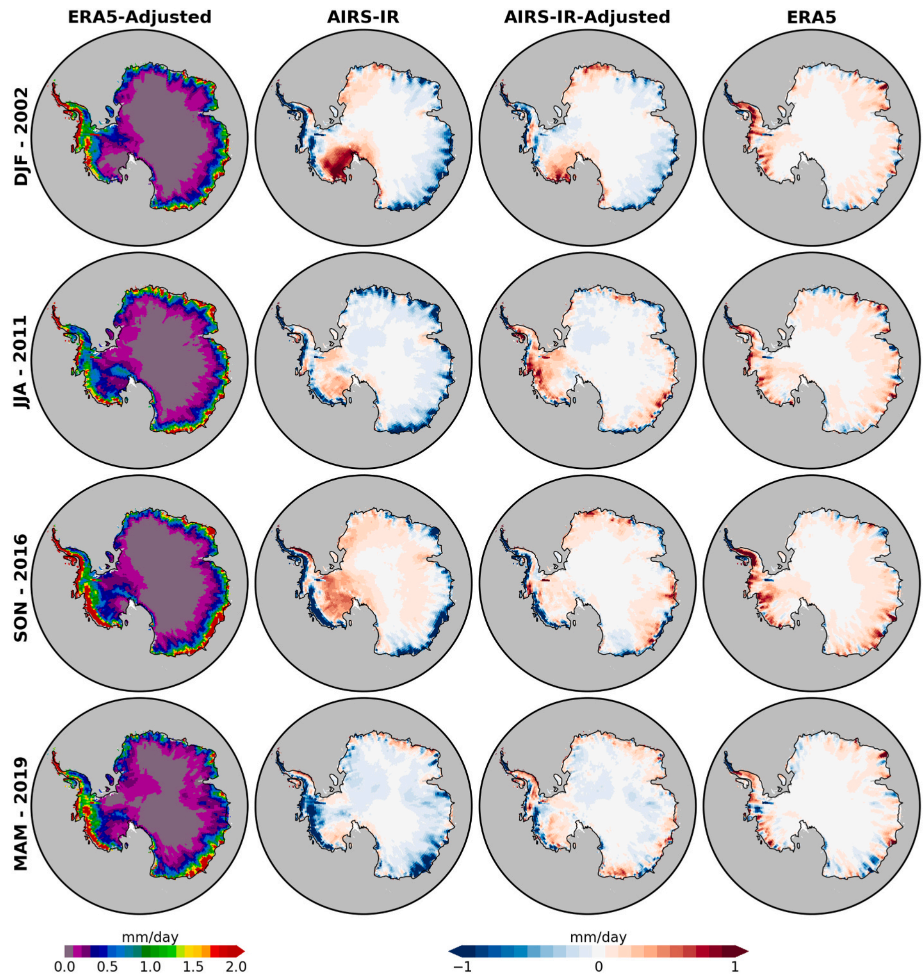

Fig. 9. Seasonal maps precipitation rates for four case studies (each for one separate season) sampled from the AIRS-IR period: First column on the left: map of precipitation from ERA5-Adjusted (i.e., the reference), second through fourth columns: Maps of precipitation values from the other products (AIRS-IR, AIRS-IR-Adjusted, ERA5) minus ERA5-Adjusted.

precipitation patterns and understand why the data record of AIRS-IR and TOVS show inconsistencies before the adjustments. For this purpose, Figs. 8 and 9 show seasonal maps of precipitation for four case studies, alongside their adjusted versions, ERA5, and ERA5-Adjusted for four different seasons sampled from different periods. In these case studies, ERA5-Adjusted serves as the reference since CloudSat and/or CloudSat-Antarctica are not available.

Fig. 8 shows that TOVS generally has a poor quality which is reflected in rather different precipitation patterns than ERA5 and ERA5-Adjusted (and CloudSat if available). Applying correction factors strongly improves the TOVS-Adjusted patterns which is also reflected in improved statistical metrics discussed later. Precipitation in the coastal regions has specifically improved. Similarly, Fig. 9 shows that applying static correction factors has greatly improved AIRS-IR precipitation maps, also confirmed by the statistical metrics in Fig. 10.

Expanding the analysis to the entire period of availability of these products, KGE, correlation coefficient, and root mean squared differences (RMSD) compared to ERA5-Adjusted are calculated for TOVS, TOVS-Adjusted, AIRS-IR, AIRS-IR-Adjusted, and ERA5. For each season, these statistics are calculated on the pixel level, and then boxplots are used to summarize the results. Note that all pixels, including those poleward of 82°S, are used for calculating the statistics since all the products completely cover Antarctica. Fig. 10 illustrates that both TOVS-Adjusted and AIRS-IR-Adjusted are more consistent with ERA5-Adjusted than their original versions, which is reflected in higher KGE and correlation coefficients, and lower RMSD (Table 2).

Since this study was motivated by deficiencies in the GPCP precipitation record over Antarctica, we compared the monthly and seasonal time series of GPCP V3.2, and GPCP-Adjusted which is constructed from TOVS-Adjusted, and AIRS-IR-Adjusted in Fig. 11. Time-series indicate that the shift in the long-term averages and variabilities between original TOVS and AIRS-IR products (Fig. 5) exist in GPCP V3.2 as well. However, GPCP constructed from TOVS-Adjusted and AIRS-IR-Adjusted (i.e., GPCP-Adjusted) does not show any obvious trends or inconsistencies in their long-term mean and variabilities. Hence, it can be concluded that the proposed approach can strongly outperform the GPCP legacy approach for adjusting TOVS and AIRS-IR using a constant scale factor. It is interesting to note that at the Antarctic-wide scale, the GPCP V3.2 and the GPCP-Adjusted show similar timing of the seasonal cycle, even at the monthly time scale, but GPCP has a much larger amplitude indicating that the proposed correction factors based on CloudSat-Antarctica product preserve temporal precipitation patterns.

3. Concluding remarks

In this study, CloudSat precipitation was used to develop a novel precipitation climatology product (called CloudSat-Antarctica) over Antarctica, where the entire surface is covered by snow and ice and current satellite-based precipitation products face major challenges. ERA5 complemented CloudSat's capabilities by mitigating some of its limitations, including poor spatiotemporal sampling, noise, and data gaps near the South Pole. The product was then used to adjust monthly

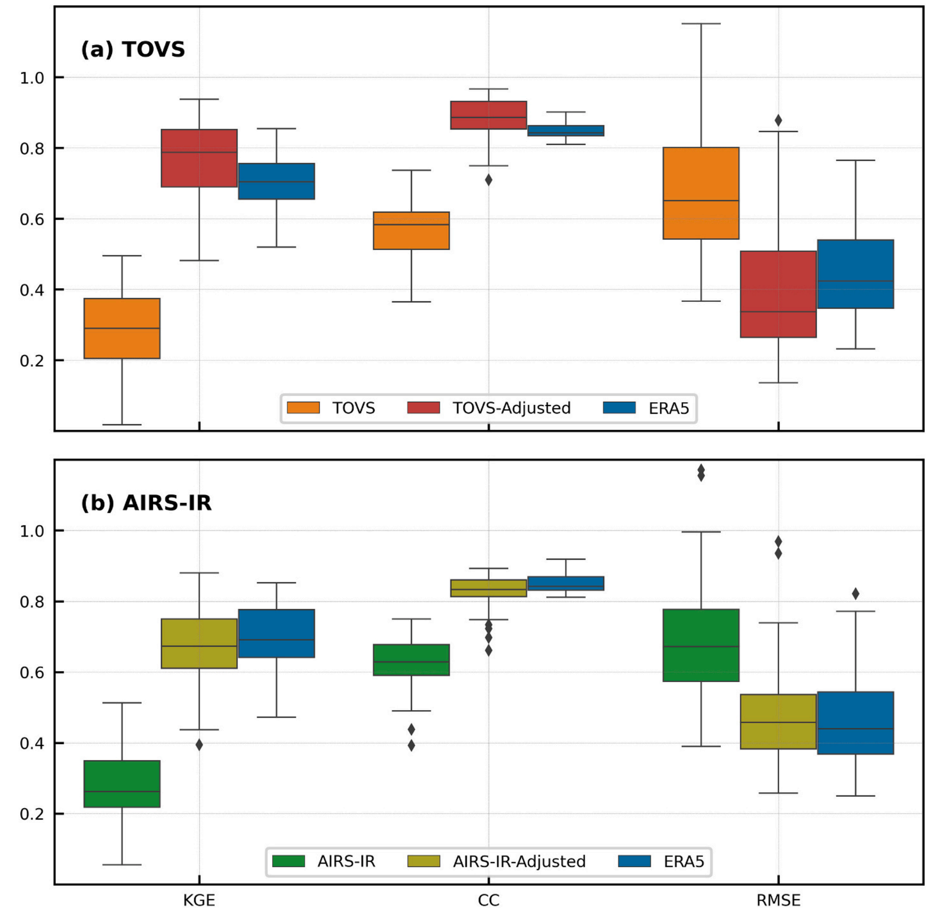

Fig. 10. Statistical metrics of the (a) TOVS and (b) AIRS-IR products compared to ERA5-Adjusted. Boxplots are constructed from the pixel-based comparison of seasonal precipitation data from TOVS, AIRS-IR, their adjusted version, and ERA5 w.r.t. ERA5-Adjusted.

Table 2
Summary of statistics for different products compared to ERA5-Adjusted.

Product	CC	KGE	RMSD [mm/day]
ERA5	0.85	0.70	0.45
AIRS	0.63	0.28	0.67
AIRS-Adjusted	0.83	0.68	0.48
TOVS	0.57	0.29	0.69
TOVS-Adjusted	0.89	0.76	0.39

TOVS and AIRS-IR precipitation biases at a pixel level because TOVS and AIRS-IR precipitation data are the sole input to the popular GPCP product over Antarctica.

Detailed investigations showed that adjusting TOVS by the climatological correction factors, derived from the overlapping period of CloudSat-Antarctica and AIRS-IR precipitation climatology, results in unreasonably large values and variations. It was found that this is mainly related to the lower quality of the TOVS precipitation product that shows an offset and slightly different pattern compared to the AIRS-IR product. Because CloudSat is not available for the TOVS period, ERA5 was adjusted with CloudSat-Antarctica and used to compute dynamic correction factors (i.e., varying monthly/seasonally) for adjusting TOVS. This was not needed for AIRS-IR, as AIRS-IR shows a pattern that compares well to CloudSat-Antarctica, so correction factors based on CloudSat-Antarctica were directly applied to AIRS-IR.

The adjusted products were evaluated through multiple analyses and cross-comparisons, including the comparison of geographical maps, and time-series of monthly and seasonal Antarctic-mean precipitation rates. The results indicate that the proposed approach can greatly improve precipitation patterns, consistency, and statistical metrics compared to the original AIRS-IR and TOVS and can be applied to other precipitation products. Consequently, this was observed in comparison of GPCP-Adjusted (constructed from TOVS and AIRS-IR Adjusted products) with the GPCP V3.2 monthly product (that uses TOVS and AIRS-IR with a constant adjustment factor over Antarctica).

The work presented here extensively used CloudSat. With the expected near-future launch and operation of the Earth, Clouds, Aerosols, and Radiation Explorer (EarthCARE) mission (Illingworth et al., 2015), such capabilities should continue, and the analysis can be updated to include additional longer-term high-quality data sets for advancing precipitation products in high latitudes. Alternatively, it is also possible to develop consistent precipitation products from the Advanced Very High Resolution Radiometer (AVHRR) sensors that cover the entire period of TOVS and AIRS. This can mitigate the TOVS issue that we faced in this work, and subsequently the dual use of ERA5 for both enhancement and assessment of the TOVS product.

CRediT authorship contribution statement

Mohammad Reza Ehsani: Writing – review & editing, Writing – original draft, Visualization, Validation, Software, Resources, Methodology, Investigation, Formal analysis, Data curation, Conceptualization. **Ali Behrangi:** Writing – review & editing, Writing – original draft, Supervision, Resources, Project administration, Funding acquisition, Conceptualization. **Cristian Román-Palacios:** Writing – review & editing, Supervision. **George J. Huffman:** Writing – review & editing, Writing – original draft, Project administration. **Robert F. Adler:**

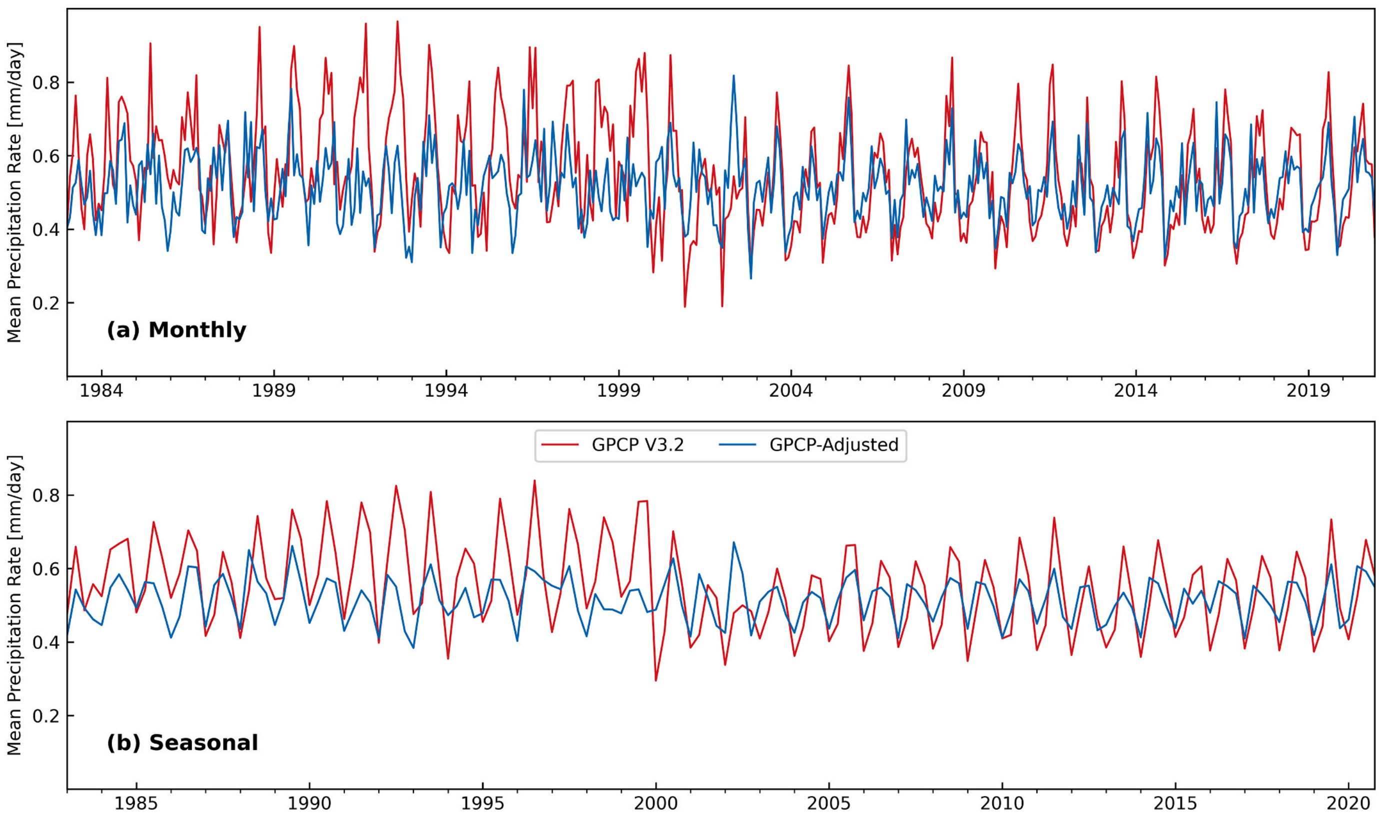

Fig. 11. (a) monthly, and (b) seasonal time series of GPCP V3.2, TOVS-Adjusted, and AIRS-Adjusted.

Writing – review & editing, Writing – original draft, Funding acquisition, Conceptualization.

Declaration of competing interest

The authors declare that they have no known competing financial interests or personal relationships that could have appeared to influence the work reported in this paper.

Data availability

GPCP V3.2 precipitation product was downloaded from the NASA Goddard Earth Sciences Data and Information Services Center (GES DISC) (https://disc.gsfc.nasa.gov/datasets/GPCPMON_3.2/summary). ERA5 data were downloaded from https://www.ecmwf.int/en/forecasts/dataset/ecmwf-reanalysis-v5. TOVS and AIRS-IR data were obtained from the GPCP team. CloudSat precipitation product was downloaded from CloudSat data processing center http://www.CloudSat.cira.colostate.edu.

Acknowledgments

The research described in this paper was carried out at the University of Arizona. Financial support is made available from NASA MEaSUREs (award numbers 80NSSC19M0006 and 80NSSC24M0018; Program Manager: Dr. Lucia Tsaoussi), and Precipitation Measurement Mission (NNH21ZDA001N-PMMST; Program Manager: Dr. Will McCarty) programs.

References

Adhikari, A., Ehsani, M.R., Song, Y., Behrangi, A., 2020. Comparative assessment of snowfall retrieval from microwave humidity sounders using machine learning methods. Earth Space Sci. 7 https://doi.org/10.1029/2020EA001357.

Arabzadeh, A., Ehsani, M.R., Guan, B., Heflin, S., Behrangi, A., 2020. Global Intercomparison of atmospheric rivers precipitation in remote sensing and reanalysis products. J. Geophys. Res. Atmos. 125 https://doi.org/10.1029/2020JD033021.

Arthern, R.J., Winebrenner, D.P., Vaughan, D.G., 2006. Antarctic snow accumulation mapped using polarization of 4.3-cm wavelength microwave emission. J. Geophys. Res. Atmos. 111 (D6) https://doi.org/10.1029/2004JD005667.

Battaglia, A., Panegrossi, G., 2020. What can we learn from the CloudSat radiometric mode observations of snowfall over the ice-free ocean? Remote Sens. 12, 3285. https://doi.org/10.3390/rs12203285.

Behrangi, A., Wen, Y., 2017. On the spatial and temporal sampling errors of remotely sensed precipitation products. Remote Sens. 9, 1127. https://doi.org/10.3390/rs9111127.

Behrangi, A., Lebsock, M., Wong, S., Lambrigtsen, B., 2012. On the quantification of oceanic rainfall using spaceborne sensors. J. Geophys. Res. Atmos. 117 https://doi.org/10.1029/2012JD017979.

Behrangi, A., Andreadis, K., Fisher, J.B., Joseph Turk, F., Granger, S., Painter, T., Das, N., 2014a. Satellite-based precipitation estimation and its application for streamflow prediction over mountainous western U.S. basins. J. Appl. Meteorol. Climatol. 53, 2823–2842. https://doi.org/10.1175/JAMC-D-14-0056.1.

Behrangi, A., Stephens, G., Adler, R.F., Huffman, G.J., Lambrigtsen, B., Lebsock, M., 2014b. An update on the oceanic precipitation rate and its zonal distribution in light of advanced observations from space. J. Clim. 27, 3957–3965. https://doi.org/10.1175/JCLI-D-13-00679.1.

Behrangi, A., Christensen, M., Richardson, M., Lebsock, M., Stephens, G., Huffman, G.J., Bolvin, D., Adler, R.F., Gardner, A., Lambrigtsen, B., Fetzer, E., 2016. Status of high-latitude precipitation estimates from observations and reanalyses. J. Geophys. Res. Atmos. 121, 4468–4486. https://doi.org/10.1002/2015JD024546.

Behrangi, A., Singh, A., Song, Y., Panahi, M., 2019. Assessing gauge Undercatch correction in Arctic basins in light of GRACE observations. Geophys. Res. Lett. 46, 11358–11366. https://doi.org/10.1029/2019GL084221.

Behrangi, A., Gardner, A.S., Wiese, D.N., 2020. Comparative analysis of snowfall accumulation over Antarctica in light of ice discharge and gravity observations from space. Environ. Res. Lett. 15, 104010 https://doi.org/10.1088/1748-9326/ab9926.

Bennartz, R., Fell, F., Pettersen, C., Shupe, M.D., Schuettemeyer, D., 2019. Spatial and temporal variability of snowfall over Greenland from CloudSat observations. Atmos. Chem. Phys. 19, 8101–8121. https://doi.org/10.5194/acp-19-8101-2019.

Berg, W., L'Ecuyer, T., Kummerow, C., 2006. Rainfall climate regimes: the relationship of regional TRMM rainfall biases to the environment. J. Appl. Meteorol. Climatol. 45, 434–454. https://doi.org/10.1175/JAM2331.1.

Broxton, P., Ehsani, M.R., Behrangi, A., 2024. Improving mountain snowpack estimation using machine learning with Sentinel-1, the airborne snow observatory, and University of Arizona snowpack data. In: Earth and Space Science, vol. 11. American Geophysical Union (AGU). https://doi.org/10.1029/2023ea002964. Issue 3.

Cabaj, A., Kushner, P.J., Fletcher, C.G., Howell, S., Petty, A.A., 2020. Constraining reanalysis snowfall over the Arctic Ocean using CloudSat observations. Geophys. Res. Lett. 47 (4) https://doi.org/10.1029/2019GL086426 e2019GL086426.

Ehsani, M.R., Behrangi, A., 2022. A comparison of correction factors for the systematic gauge-measurement errors to improve the global land precipitation estimate. J. Hydrol. (Amst) 610, 127884. https://doi.org/10.1016/j.jhydrol.2022.127884.

Ehsani, M.R., Behrangi, A., Adhikari, A., Song, Y., Huffman, G.J., Adler, R.F., Bolvin, D. T., Nelkin, E.J., 2021. Assessment of the advanced very high-resolution radiometer (AVHRR) for snowfall retrieval in high latitudes using CloudSat and machine learning. J. Hydrometeorol. 22, 1591–1608. https://doi.org/10.1175/jhm-d-20-0240.1.

Ehsani, M.R., Heflin, S., Risanto, C.B., Behrangi, A., 2022a. How well do satellite and reanalysis precipitation products capture the North American monsoon season in Arizona and New Mexico? Weather Clim. Extrem. 38, 100521 https://doi.org/10.1016/j.wace.2022.100521.

Ehsani, M.R., Zarei, A., Gupta, H.V., Barnard, K., Lyons, E., Behrangi, A., 2022b. NowCasting-Nets: representation learning to mitigate latency gap of satellite precipitation products using convolutional and recurrent neural networks. IEEE Trans. Geosci. Remote Sens. 60, 1–21. https://doi.org/10.1109/TGRS.2022.3158888.

Ferraro, R.R., Peters-Lidard, C.D., Hernandez, C., Turk, F.J., Aires, F., Prigent, C., Lin, X., Boukabara, S.-A., Furuzawa, F.A., Gopalan, K., Harrison, K.W., Karbou, F., Li, L., Liu, C., Masunaga, H., Moy, L., Ringerud, S., Skofronick-Jackson, G.M., Tian, Y., Wang, N.-Y., 2013. An evaluation of microwave land surface emissivities over the continental United States to benefit GPM-era precipitation algorithms. IEEE Trans. Geosci. Remote Sens. 51, 378–398. https://doi.org/10.1109/TGRS.2012.2199121.

Ghajarnia, N., Akbari, M., Saemian, P., Ehsani, M.R., Hosseini-Moghari, S., Azizian, A., Kalantari, Z., Behrangi, A., Tourian, M.J., Klöve, B., Haghighi, A.T., 2022. Evaluating the evolution of ECMWF precipitation products using observational data for Iran: from ERA40 to ERA5. Earth Space Sci. 9 https://doi.org/10.1029/2022EA002352.

Grazioli, J., Madeleine, J.-B., Gallée, H., Forbes, R.M., Genthon, C., Krinner, G., Berne, A., 2017. Katabatic winds diminish precipitation contribution to the Antarctic ice mass balance. Proc. Natl. Acad. Sci. 114, 10858–10863. https://doi.org/10.1073/pnas.1707633114.

Hersbach, H., Bell, B., Berrisford, P., Hirahara, S., Horányi, A., Muñoz-Sabater, J., Nicolas, J., Peubey, C., Radu, R., Schepers, D., Simmons, A., Soci, C., Abdalla, S., Abellan, X., Balsamo, G., Bechtold, P., Biavati, G., Bidlot, J., Bonavita, M., De Chiara, G., Dahlgren, P., Dee, D., Diamantakis, M., Dragani, R., Flemming, J., Forbes, R., Fuentes, M., Geer, A., Haimberger, L., Healy, S., Hogan, R.J., Hólm, E., Janisková, M., Keeley, S., Laloyaux, P., Lopez, P., Lupu, C., Radnoti, G., de Rosnay, P., Rozum, I., Vamborg, F., Villaume, S., Thépaut, J.N., 2020. The ERA5 global reanalysis. Q. J. R. Meteorol. Soc. 1999–2049 https://doi.org/10.1002/qj.3803.

Hoopes, C.A., Castro, C.L., Behrangi, A., Ehsani, M.R., Broxton, P., 2023. Improving prediction of mountain snowfall in the southwestern United States using machine learning methods. In: Meteorological Applications, vol. 30. Wiley. https://doi.org/10.1002/met.2153. Issue 6.

Huffman, G.J., Bolvin, D.T., Braithwaite, D., Hsu, K., Joyce, R., Kidd, C., Nelkin, E.J., Sorooshian, S., Stocker, E.F., Tan, J., Wolff, D.B., Xie, P., 2020. In: Levizzani, V., Kidd, C., Kirschbaum, D., Kummerow, C., Nakamura, K., Turk, F.J. (Eds.), Integrated Multi-satellitE Retrievals for the Global Precipitation Measurement (GPM) mission (IMERG). Chapter 19 in Adv. Global Change Res., Vol. 67, Satellite Precipitation Measurement. Springer Nature, Dordrecht, pp. 343–353. https://doi.org/10.1007/978-3-030-24568-9_19. ISBN 978–3–030-24567-2 / 978–3–030–24568-9 (eBook).

Huffman, G.J., Adler, R.F., Behrangi, A., Bolvin, D.T., Nelkin, E.J., Gu, G., Ehsani, M.R., 2023. The new version 3.2 Global Precipitation Climatology Project (GPCP) monthly and daily precipitation products. J. Clim. 36, 7635–7655. https://doi.org/10.1175/JCLI-D-23-0123.1.

Illingworth, A.J., Barker, H.W., Beljaars, A., Ceccaldi, M., Chepfer, H., Clerbaux, N., Cole, J., Delanoë, J., Domenech, C., Donovan, D.P., Fukuda, S., Hirakata, M., Hogan, R.J., Huenerbein, A., Kollias, P., Kubota, T., Nakajima, T., Nakajima, T.Y., Nishizawa, T., Ohno, Y., Okamoto, H., Oki, R., Sato, K., Satoh, M., Shephard, M.W., Velázquez-Blázquez, A., Wandinger, U., Wehr, T., van Zadelhoff, G.-J., 2015. The EarthCARE satellite: the next step forward in global measurements of clouds, aerosols, precipitation, and radiation. Bull. Am. Meteorol. Soc. 96, 1311–1332. https://doi.org/10.1175/BAMS-D-12-00227.1.

Kidd, C., Huffman, G., 2011. Global precipitation measurement. Meteorol. Appl. 18, 334–353. https://doi.org/10.1002/met.284.

King, F., Fletcher, C.G., 2021. Using CloudSat-derived snow accumulation estimates to constrain gridded snow water equivalent products. Earth Space Sci. 8 (10) https://doi.org/10.1029/2021EA001835 e2021EA001835.

Kulie, M.S., Milani, L., Wood, N.B., Tushaus, S.A., Bennartz, R., L'Ecuyer, T.S., 2016. A shallow cumuliform snowfall census using spaceborne radar. J. Hydrometeorol. 17, 1261–1279. https://doi.org/10.1175/JHM-D-15-0123.1.

Kummerow, C., Olson, W.S., Giglio, L., 1996. A simplified scheme for obtaining precipitation and vertical hydrometeor profiles from passive microwave sensors. IEEE Trans. Geosci. Remote Sens. 34, 1213–1232. https://doi.org/10.1109/36.536538.

Lebsock, M.D., L'Ecuyer, T.S., 2011. The retrieval of warm rain from CloudSat. J. Geophys. Res. 116, D20209. https://doi.org/10.1029/2011JD016076.

Liu, G., 2008. Deriving snow cloud characteristics from CloudSat observations. J. Geophys. Res. 113, D00A09. https://doi.org/10.1029/2007JD009766.

Milani, L., Wood, N.B., 2021. Biases in CloudSat falling snow estimates resulting from daylight-only operations. Remote Sens. 13 (11) https://doi.org/10.3390/rs13112041. Article 11.

Palerme, C., Kay, J.E., Genthon, C., L'Ecuyer, T., Wood, N.B., Claud, C., 2014a. How much snow falls on the Antarctic ice sheet? Cryosphere 8, 1577–1587. https://doi.org/10.5194/tc-8-1577-2014.

Palerme, C., Kay, J.E., Genthon, C., L'Ecuyer, T., Wood, N.B., Claud, C., 2014b. How much snow falls on the Antarctic ice sheet? Cryosphere 8 (4), 1577–1587. https://doi.org/10.5194/tc-8-1577-2014.

Palerme, C., Genthon, C., Claud, C., Kay, J.E., Wood, N.B., L'Ecuyer, T., 2017. Evaluation of current and projected Antarctic precipitation in CMIP5 models. Clim. Dyn. 48, 225–239. https://doi.org/10.1007/s00382-016-3071-1.

Sadeghi, M., Akbari Asanjan, A., Faridzad, M., Afzali Gorooh, V., Nguyen, P., Hsu, K., Sorooshian, S., Braithwaite, D., 2019. Evaluation of PERSIANN-CDR constructed using GPCP V2.2 and V2.3 and a comparison with TRMM 3B42 V7 and CPC unified gauge-based analysis in global scale. Remote Sens. 11, 2755. https://doi.org/10.3390/rs11232755.

Schneider, U., Finger, P., Meyer-Christoffer, A., Rustemeier, E., Ziese, M., Becker, A., 2017. Evaluating the hydrological cycle over land using the newly-corrected precipitation climatology from the Global Precipitation Climatology Centre (GPCC). Atmosphere (Basel) 8. https://doi.org/10.3390/atmos8030052.

Seefeldt, M.W., Low, T.M., Landolt, S.D., Nylen, T.H., 2021. Remote and autonomous measurements of precipitation for the northwestern Ross Ice Shelf, Antarctica. Earth Syst. Sci. Data 13 (12), 5803–5817. https://doi.org/10.5194/essd-13-5803-2021.

Seto, S., Iguchi, T., Meneghini, R., 2022. Correction of path-integrated attenuation estimates considering the soil moisture effect for the GPM dual-frequency precipitation radar. J. Atmos. Ocean. Technol. 39, 803–821. https://doi.org/10.1175/JTECH-D-21-0111.1.

Skofronick-Jackson, G., Kulie, M., Milani, L., Munchak, S.J., Wood, N.B., Levizzani, V., 2019. Satellite estimation of falling snow: a global precipitation measurement (GPM) Core Observatory perspective. J. Appl. Meteorol. Climatol. 58, 1429–1448. https://doi.org/10.1175/JAMC-D-18-0124.1.

Smalley, M., Kirstetter, P.-E., L'Ecuyer, T., 2017. How frequent is precipitation over the contiguous United States? Perspectives from ground-based and spaceborne radars. J. Hydrometeorol. 18, 1657–1672. https://doi.org/10.1175/JHM-D-16-0242.1.

Song, Y., Broxton, P.D., Ehsani, M.R., Behrangi, A., 2021. Assessment of snowfall accumulation from satellite and reanalysis products using SNOTEL observations in Alaska. Remote Sens. 13, 2922. https://doi.org/10.3390/rs13152922.

Stephens, G.L., Vane, D.G., Boain, R.J., Mace, G.G., Sassen, K., Wang, Z., Illingworth, A. J., O'connor, E.J., Rossow, W.B., Durden, S.L., Miller, S.D., Austin, R.T., Benedetti, A., Mitrescu, C., 2002. The CLOUDSAT mission and the A-Train. Bull. Am. Meteorol. Soc. 83, 1771–1790. https://doi.org/10.1175/BAMS-83-12-1771.

Sun, Q., Miao, C., Duan, Q., Ashouri, H., Sorooshian, S., Hsu, K., 2018. A review of global precipitation data sets: data sources, estimation, and Intercomparisons. Rev. Geophys. 56, 79–107. https://doi.org/10.1002/2017RG000574.

Susskind, J., Piraino, P., Rokke, L., Iredell, L., Mehta, A., 1997. Characteristics of the TOVS Pathfinder Path A dataset. Bull. Am. Meteorol. Soc. 78, 1449–1472. https://doi.org/10.1175/1520-0477(1997)078<1449:COTTPP>2.0.CO;2.

Tanelli, S., Durden, S.L., Im, E., Pak, K.S., Reinke, D.G., Partain, P., Haynes, J.M., Marchand, R.T., 2008. CloudSat's cloud profiling radar after two years in orbit: performance, calibration, and processing. IEEE Trans. Geosci. Remote Sens. 46, 3560–3573. https://doi.org/10.1109/TGRS.2008.2002030.